Working Paper

Space-time Dynamics of Urban Systems from Satellite Images of Night Lighting. Economic Scenarios for European Metropolitan Regions

Metropolitan Laboratory of Ecology and Territory of Barcelona

Project CP_2019_6.2.1

December 2019

Title Page

Space-time Dynamics of Urban Systems revealed using Satellite Images of Night Lighting. Economic Scenarios for European Metropolitan Regions

Aureli Alabert[a], Joan Marull[b,*], Albert Ruiz[a], Francesc Coll[b], Maria Miranda[a], Roc Padró[b]

[a] Department of Mathematics, Autonomous University of Barcelona, E-08193 Bellaterra, Spain.

[b] Barcelona Institute of Regional and Metropolitan Studies, Autonomous University of Barcelona, E-08193 Bellaterra, Spain.* Corresponding author: Tel: +34 935868880; Email: joan.marull@uab.cat

Acknowledgements

This research was carried out at the Metropolitan Laboratory of Ecology and Territory of Barcelona (LET) and was commissioned by the Barcelona Metropolitan Area (project CP_2019_6.2.1).

Abstract

The aim of this study was to use satellite imagery of metropolitan regions and historical data to develop a method for predicting the evolution of Night-Time Light (NTL) and design a mathematical Cellular Automata (CA) model to predict urban scenarios. In order to calibrate and validate the CA model with real data, we used NTL data for 1992–2012 from the European NUTS-2 region of Catalonia. *Lighted surface* scenarios (as an estimate of urban expansion) were calculated using variations in *light intensity* (as an estimate of economic activity). In all, we applied the CA model to twelve NUTS-3 European metropolitan regions (Amsterdam, Barcelona, Brussels, Hamburg, London, Lyon, Madrid, Milan, Munich, Paris, Rome and Vienna). The CA model behaved as expected, in the sense that it was sensitive to increases in NTL. As this parameter is directly related to Gross Domestic Product (GDP), the model thus allows us to calculate urban growth scenarios in relation to economic activity. Since NTL is available for the entire globe, the CA model could be used to study urbanization dynamics in metropolitan regions for which, in particular, socio-economic data is not available at this territorial scale, and even megaregions emerging as global economic units.

Key words

Urban Growth, Cellular Automata, Satellite Datasets, Regional Modelling, Metropolis, Europe

1. Introduction

Ever since the nineteenth century, when industrial cities first began to emerge, urban areas around the world have continued to expand and increase their complexities (Batty 2011). This has posed important problems when dealing with, assessing and understanding phenomena such as changes in land-use, transportation, economic growth and environmental sustainability (Barreira-González et al 2015). Owing to their great complexity, as yet these problems are neither fully understood nor satisfactorily resolved (Batty 2015). However, it seems clear that contemporary cities are the outcome of complex, open social systems of interacting human agents subject to the effects of several endogenous factors and exogenous constraints (e.g. cognitive, cultural, economic, technological, environmental and social). Almost all of these factors and constraints involve networks of relationships between individuals, groups, institutions and whole societies, which give rise to feedback loops of information that ensure that the understanding and simulation of all these interactions and relevant systems is highly complex (Portugali 2011, Ioannides 2012).

From a macroscopic point of view (i.e. at the level of urban observables such as GDP, number of patents, electrical consumption and road surface area), it is not yet known whether any city variables transcend their contextual constraints (i.e. do these measures obey universal laws other than the refuted scaling laws?) (Arcaute et al. 2015). On the other hand, a trend towards the microscopic view of cities has emerged due to awareness of the inadequacy of the original centralized, top-down, static paradigm for modelling and planning urban systems, and to the growing need to consider interacting entities at different scales. This realization arose during the final quarter of the twentieth century and provoked a move towards a more decentralized, disaggregated, bottom-up, self-organizing and dynamic approach to simulating urban phenomena (Allen 1997, Portugali 2000). In this context a new generation of urban models based on Cellular Automata (CA) (Clarke et al. 1997, White and Engelen 2000, Santé et al. 2010) and agents in general (Benenson and Torrens 2004, Rai and Robinson 2015) began to emerge.

On a microscopic scale (i.e. at the level of human interactions) agent-based models are used to simulate population dynamics. At a mesoscopic or coarse scale corresponding to the level of interacting entities without explicit consideration of the interactions of human agents, CA modelling of land-use dynamics are able to describe how the relatively slow changes in the physical structure of the city take place (Benenson 1999).

Furthermore, the quest for accurate simulations of urban systems has led to the use of integrated models at different levels involving exogenous constraints (White 2006, Van Vliet et al. 2012) and networks of relationships (Benenson 1999), a combination that takes place within the context of Portugali's cities of free agents in a cellular space (Portugali 2000). Nevertheless, these ideas are still in their infancy (Batty 2005).

In this context, despite – and also because of – the great complexity of urban systems, we decided to investigate whether or not it is possible to obtain useful information – albeit necessarily approximate (Van der Leeuw 2004) – about urban land dynamics using Night-Time Light (NTL) satellite imagery as the single input into a CA-based model with coarse cell space. This approach was motivated by the fact that NTL is a proxy of several urban observables (e.g. population, GDP and energy consumption) (Marull et al. 2013). We have developed a CA-based model for urban landscape changes using a non-standard CA that is typical of urban CA-based models (Couclelis 1985, White and Engelen 1997). A standard CA consists of a homogeneous grid whose cell space is characterized and configured at any time by a finite set of states. This configuration changes in discrete time steps according to a time and space invariant transition rule operating on each cell, and depending upon the previous states of a uniformly defined neighbourhood.

In summary, CA would seem to be a suitable technique for this task since it involves evolution over time possibly influenced by spatial proximity. This technique has been used to model urban growth using several variables (Liu 2009, Guan et al. 2011, Al-shalabi et al. 2013, Barreira-González et al 2015) but not with NTL lighting imagery. Even so, this type of image has been used in the context of energy consumption to evaluate the extension and intensity of the urban expansion (Nel·lo et al. 2017) and urban sustainable progress (Marull et al. 2019) in Western Europe. The goal of this paper is thus to propose a method for predicting the evolution of NTL in European metropolitan regions based on historical data to calibrate a mathematical CA model and predict urban scenarios.

To generate this mathematical model and, above all, to analyze future scenarios for urban progress, we simulated NTL variation using a theoretically based and heuristically driven constrained CA model for a European Union NUTS-2 region (Catalonia, NE Spain). We focussed on two definite macroscopic variables: *lighted surface* and *light intensity*. Defining the transition rules is the core problem to be solved when developing a CA model. We used an inverse and heuristic approach starting from data analysis (Rabino and Laghi 2002).

The resulting transition rules are not stochastic nor affected by distance decay, as expected in urban systems (White and Engelen 2000), but, rather, depend upon the previous states of cell neighbours. These rules also depend upon additional variables that determine the type of transition. In order to calibrate and validate the model with real data (Engelen and White 2008), we used NTL data for 1992–2012 from the NUTS-2 region of Catalonia. Finally, *lighted surface* scenarios (as a proxy of urban expansion) are expressed as variations in *light intensity* (as a proxy of GDP dynamics) imposed exogenously on different NUTS-3 European metropolitan regions: *Amsterdam*, *Barcelona*, *Brussels*, *Hamburg*, *London*, *Lyon*, *Madrid*, *Milan*, *Munich*, *Paris*, *Rome* and *Vienna*.

2. Materials and Methods

2.1. Satellite Images of Night Lighting

Night-time light (NTL) data detected by artificial satellites allow us to analyse on a global scale the evolution of city networks towards structures exceeding metropolitan scale (Zhang and Seto 2011) that can be defined as metropolitan regions or even megaregions (Marull et al. 2013). Applications developed using NTL data (Doll 2008) enable us to delineate urban extensions, calculate energy consumption, estimate economic activity, and model greenhouse gas emissions at regional level.

The main database used for developing an urban CA model comprises the series of images produced by DMSP-OLS sensors and freely distributed by the National Geophysical Data Center of National Oceanic and Atmospheric Administration (NOAA). These images are in GeoTiff format and have a spatial resolution of approximately 1 km^2 per pixel (30'). Each pixel sensor of the satellite is assigned a specific value of light intensity as a DN (Digital Number) with a radiometric resolution of 6 bits that can vary between 0 and 63. Given that metropolitan regions are areas characterized by great physical contiguity in human settlements, NTL data has been used as a proxy for urban expansion (Nel·lo et al 2017). Using this methodological procedure for an annual series of data (1992–2012), we developed and tested the model in a European NUTS-2 region, and then measured the simulated evolution of different metropolitan regions in the European Union.

The European NUTS-2 region used for testing the model (Fig. 1) included the intensities of NTL in a rectangular area that covered Catalonia (NE Spain) with a 15-km buffer on all four sides. The area was divided

into approximately 1-km^2 cells, each with its own NTL intensity recorded annually in 1992–2012. Each cell was identified by the coordinates of its centroid and its NTL intensity was denoted by a number between 0 and 63. The study area embraced the whole of Catalonia. Each cell was marked as belonging either to this region, to another territory (Spain or France) or to the sea. We also used the percentage of cell corresponding to i) Natural Protected Areas, ii) Slope > 20%, iii) Water Bodies, iv) Floodable Areas, and v) Sea, which necessarily had null or almost null illumination because theoretically there is no urban development in these areas and so no tendency to increase. To cope with this limitation, we defined a *capacity* (maximum allowed intensity), which was also a number between 0 and 63. The *intensity* of a cell in a given year was a number between 0 and its *capacity*.

European metropolitan regions are NUTS-3 regions or a combination of NUTS-3 regions that represent agglomerations of at least 250,000 inhabitants. These conglomerations were identified using the Larger Urban Zones in the Urban Audit (https://ec.europa.eu/regional_policy/en/) and each was represented by at least one NUTS-3 region. If in an adjacent NUTS-3 region more than 50% of the population also lived within this agglomeration, it was included in the metropolitan region. We selected the following European metropolitan regions (Fig. 2) to apply the model (EU code): *Amsterdam* (NL002MC), *Barcelona* (ES002M), *Brussels* (BE001MC), *Hamburg* (DE002M), *London* (UK001MC), *Lyon* (FR003M), *Madrid* (ES001MC), *Milan* (IT002M), *Munich* (DE003M), *Paris* (FR001MC), *Rome* (IT001MC) and *Vienna* (AT001MC).

2.2. Space-time Dynamics of Urban Systems

2.2.1. Cellular Automata (CA)

CA are mathematical models that describe the evolution over time of a set of entities with a spatial internal relationship. The constitutive elements of a cellular automaton are: i) the cell: the basic spatial unit; ii) the states: there is a set of possible states such that at any point in time all cells are in one of these possible states; iii) the neighbourhood: the spatial distribution of the cells gives rise to a notion of proximity and cells that are 'close' in some sense to a given cell constitute its neighbourhood; iv) the time, which evolves in a discrete manner; v) the transition rule that determines how the state of a cell changes from one point in time to the next one as a function of the current state of the cell and that of its neighbouring cells.

CA are flexible models. Cells, states and time are usually largely determined by the specific situation under study. However, the neighbourhood and the transition rules can be chosen in a freer way and so there is some leeway for selecting parameters that configure the automaton's behaviour.

Geographical information that evolves over time (yearly, monthly, weekly) is clearly suitable for modelling by CA. Indeed, the information (*states*) are related to points or small pieces of land (*cells*) on a given area of the Earth's surface. As well, there is an intuitive notion of distance (although several variants can be used) and so the notion of the neighbourhood of each cell – as a set of other such cells – can be defined based on distance. Finally, depending on the information being employed, the state of a cell at time $t + 1$ may well be influenced by the states of nearby cells at time t, giving rise to local interactions.

CA also feature a dimension, which is simply the spatial dimension of the array of cells. In our case, the dimension is 2, since we are analyzing a segment of the Earth's surface, which we can think of as being projected onto a Euclidean plane. Classically, the cells in two-dimensional CA models are simply equal-sided squares and the neighbourhood is defined by the concept of layer. The 1-layer of a square cell is the set of eight cells that share a side or a vertex with it. The 2-layer is the set of sixteen cells which are in contact with the 1-layer, and so on. Hexagons are also used sometimes since they tessellate the plane and also seem to respect a little more the intuition of the usual (Euclidean) distance when considering layers. Indeed, the six 1-layer cells in a hexagonal tessellation all have one side in common with the central cell, whereas with squares, those in the cardinal directions are closer to the central cell than the others.

In this paper, we abandon the layer concept. We use a model of neighbourhood that fully respects the notion of Euclidean distance: all points at the same distance from the central point of a cell will have the same influence on the evolution of the cell. As far as we know, this is a novel procedure in CA models, which we chose because we specifically did not want to consider obstacles or pathways and only wanted to assess the impact of the neighbourhood as a function of the straight line distance.

Concerning the transition rule, the state $S_i(t + 1)$ of a cell i at time $t + 1$ is usually determined by some function f of the states of the cells in its neighbourhood N_i (eq. 1):

Eq. 1 $$S_i(t + 1) = f\big(S_j(t),\ j \in N_i\big)$$

For instance, in the classical (two-dimensional) Conway's 'Game of Life' (Gardner 1970), one of the first CAs to be studied, the states of the cells are 0 or 1. A cell at state 1, with two or three neighbours at state 1, will remain at state 1 in the next period; a cell at state 0, with precisely three neighbours at state 1, will change to state 1; in any other case, the cell will be at state 0 in the next period. This simple rule gives a surprising richness of evolutionary behaviour that depends on the initial state of the cells. It should be emphasized that Equation 1 above implies that the change in state is synchronous, that is, all cells change at the same time.

We can consider that a cell belongs to its own neighbourhood or not. For our purposes, it is simpler to think that the cell does not belong to its neighbourhood. We will consider the present state of a cell separately. This is only a formal distinction that helps present the model and its possible extensions.

An important element that a transition rule must specify is how to treat the boundary of the set of cells. Theoretically, we would like to apply the same formula to all cells. However, cells near the boundary pose a problem. They do not have the same number of neighbours as the interior cells; therefore, the transition rule must be defined specifically for the close-to-boundary cells, whether the concept of layer is used or not.

If we had an infinite plane, the boundary naturally would not be a problem. With a bounded domain, you can, for instance, consider the cellular structure of a torus ('if you leave from one side, you re-enter from the opposite side') or of other boundaryless topological objects; nevertheless, this is clearly not an option (unless you are taking into consideration the entire planet!) since we want to apply the structure to a real region. We believe that our approach to the boundary problem is original and was to some extent forced by the need to preserve the total illumination of the study region, as we will see later.

2.2.2. Application to light intensity evolution

Our aim was to use a CA to mimic the observed evolution of the NTL intensity of a cell in the period 1992–2012 as recorded in the satellite data at our disposal. A logical first step was to assign each geographical cell for which we have an annual value of NTL intensity a single cell in the CA.

Typically, in a CA cells can take any of the values of the set of states. In our case, many of the cells have a capacity that is less than the general upper limit. Our set of states is the real interval of numbers $[0,63]$, but the cells i with limited capacity M_i can only take a value in the interval $[0, M_i]$. An extreme example are the cells

in the sea, far from the coast, which must have a capacity $M_i = 0$. The definition of the transition rule has to take this fact into account.

Once it is clear how to model the cells, states and time in our real case, it still remains to determine suitable neighbourhood and transition rule definitions. As commented above, our intention is to build a model that uses the straight-line distance between geographical points, irrespective of the existence of roads or natural barriers. Thus, we defined the neighbourhood of a cell in a way that most respects this idea. Moreover, this led us to abandon the concept of layers.

Specifically, we defined the neighbourhood of a cell as consisting of all the cells that wholly or partially lie inside a circle whose centre is the mid-point of the cell (the centroid of the square) at a radius $r>0$. This definition will be modified for the cells near the boundary, as we shall see. For the moment, let's consider only the generic case. Not all the cells in the neighbourhood will have the same impact on the future state of the central cell and we'd like in some way for this impact to decrease with distance. The transition rule will model this.

Let's consider a non-negative function $f: R^2 \to R$ that we will call the 'kernel' of the sequel, with circular symmetry around its centre, decreasing in any radial direction, and with a finite total volume enclosed between the function surface and the horizontal plane. An example of such a function is the two-dimensional Gaussian probability density. We need the support of the function to be bounded; hence a proper Gaussian density is not a good candidate. However, it can be modified by truncation and so it qualifies. We have used this truncated Gaussian and a cone-shaped function, supported on a circle, that features a linearly decreasing value from the centre to the points at a distance r, where it vanishes. Details are given below.

Once a kernel function is fixed, we can consider a given cell with its centroid located at the origin of the Euclidean plane, and compute the volume under the surface of the graph of the function f, enclosed by each cell in its neighbourhood. The proportion of the volume that each neighbouring cell encloses (discounting the central cell itself, which we will consider separately) will be regarded as a weight coefficient and taken to have a nominal contribution independent of distance.

The nominal contribution of each neighbouring cell can be computed in the following way: let $I_i \coloneqq S_i(t)$ denote the present intensity in cell i, and $I_j \coloneqq S_j(t)$ the present intensity in a cell j belonging to the

neighbourhood of i. The proportion of intensities with respect to the capacities of these cells is therefore $p_i = \frac{I_i}{M_i}$ and $p_j = \frac{I_j}{M_j}$, respectively. This difference in proportions somehow measures the 'pressure' that the cell with the larger proportion exerts on the other cell. This will determine the direction of the transfer of light intensity; the amount of transfer will be proportional to the difference between the proportions. The amount will also be proportional to the intensity difference in an absolute value. Denoting $w_j(i)$ to be the weight given by the kernel function to cell j when contributing to cell i, we find that the amount of transfer from cell j to cell i will be, theoretically,

$$w_j(i)\left(p_j - p_i\right)\left|I_j - I_i\right|$$

which can be positive or negative.

We have to introduce several restrictions to this quantity. If the transfer is positive, it cannot be greater than the difference $M_i - I_i$ of the capacity and the current intensity of i, and it cannot be greater than the current intensity I_j of j. Analogously, if the transfer is negative, it cannot be less than $-\left(M_j - I_j\right)$ and $-I_i$. Summing up for all cells j in the neighbourhood N_i of cell i, and denoting again $S_i(t) \coloneqq I_i$, we get the following formula (eq. 2) for the contribution of the neighbours of cell i at time t:

$$\text{Eq. 2} \qquad C_i(t) = S_i(t) + \sum_{j \in N_i} w_j(i)\left(p_j(t) - p_i(t)\right)\left|S_j(t) - S_i(t)\right|$$

$$\wedge \left(M_i - S_i(t)\right) \wedge S_j(t) \vee -\left(M_j - S_j(t)\right) \vee -S_i(t)$$

where $\wedge$ and $\vee$ are the supremum and the infimum operators, respectively.

We excluded cell i from the CA contribution because we want to consider it separately. This will facilitate the description and help interpret our results. Consider now a value $\lambda \in [0,1]$ and the definition of the predicted state (intensity) of cell i at time $t+1$ as follows (eq. 3):

$$\text{Eq. 3} \qquad S_i(t+1) = \lambda S_i(t) + (1-\lambda) C_i(t)$$

where $C_i(t)$ has been computed in formula (eq. 2). In other words, our transition rule is a convex combination of the present value of the cell in question and the contribution of its neighbours. Instead of the present value, one can also consider a value that takes into account the past tendency of the cell; this will be discussed later but not as part of the analyses.

Equation 3 will still be modified by the growth factors (see below).

2.2.3. The model parameters

The above formula contains several parameters; one is apparent, the convex coefficient λ, and the other two hidden, the choice of the function f in Equation 1 supported on a circle, and the radius r of that circle.

There are infinitely many functions f with the desired properties and we shall consider two of them. One gives slightly better results than the other, although the difference is not great. The first function is the truncated Gaussian that, given a radius r, is the centred Gaussian probability density with a diagonal covariance matrix such that the probability (volume under the surface) of the circle of radius r is equal to 0.99. The function is set to zero outside the circle. There is no need to normalise the function to a probability density since the cells will simply take the proportion of volume they contain so that all weights $w_j(i)$ add up to 1. Thus, this function is given by the mapping

$$(x, y) \mapsto \frac{1}{2\pi\sigma^2} exp \frac{x^2 + y^2}{2\sigma^2}, \quad x^2 + y^2 \leq r^2$$

The variance σ^2 is a function of the intended radius r according to

$$\sigma^2 = \frac{-r^2}{2\ log\ (0.01)}$$

The second function considered is a cone-shaped function with an enclosing volume = 1. Given the radius r, the function is defined by

$$(x, y) \mapsto \frac{3}{\pi r^2}\left(1 - \sqrt{\frac{x^2 + y^2}{r^2}}\right), \quad x^2 + y^2 \leq r^2$$

To summarize, we have the freedom to choose λ, f and r and so make the evolution of the predictions as similar as possible to the observed values, according to certain criteria. This leads us to an optimisation problem: we want to find λ, f and r to ensure that the predictions are as close as possible to the real data. These optimal values can then be applied to predict the future evolution of the system.

2.2.4. The growth factors

Before turning to the optimisation problem itself, let's examine one more element contained in the data: the growth factors.

In an Appendix we prove that the evolution according to Equation 3 keeps the total intensity of the map constant over time. However, we can compute the sum of the intensities of all the cells, which, of course, will be different every year; indeed, we can interpret the ratio between successive total intensities as an indicator of economic growth, which can be either greater (economic expansion) or less (economic contraction) than 1. Therefore, to realistically model past evolution, the increase or decrease in total light intensity should be taken into account. When predicting the future evolution, these growth factors must be substituted supplied, giving rise to different scenarios, according to different hypotheses of economic evolution.

The growth factor can vary from one area to another if the study region is large. To keep things simple here, we employ a uniform growth factor throughout the whole study region. Therefore, we apply this factor $G(t)$ given by

$$G(t) := \frac{\sum_i S_i(t+1)}{\sum_i S_i(t)}$$

to all cells on the map, thus getting the transition rule (eq. 4)

Eq. 4 $$S_i(t+1) = G(t)\big(\lambda S_i(t) + (1-\lambda)C_i(t)\big)$$

When the growth factor is less than 1, there are no further problems. If it is greater than 1, however, we have to deal with the possibility of cells reaching a light intensity that is beyond their capacity. In this case, it is natural that this surplus is spread in some way towards nearby cells.

The left-over intensity of a cell is spread first to the neighbouring cells that are below their maximum. If after this redistribution there is still some surplus intensity, we have to check the second layer of neighbouring cells and repeat the procedure with the same conditions (i.e. the intensity is added to each cell that is below its maximum; more intensity than the cell can assume is not assigned). This procedure continues for as long as there is left-over intensity in the initial cell. The implemented algorithm has the following properties: i) assuming the amount of light in the system is less than its total capacity, the algorithm stops after a finite number of steps; ii) the algorithm does not depend on the order in which we check the cells that have more light than their capacity.

2.2.5. The boundary of the cellular automaton

The problem with the cells near the boundary is that the transition rule has to be adapted to the fact that these cells possess fewer neighbours within a distance less than r.

Our aim is to obtain a transition rule that for a growth factor $G = 1$ preserves the total intensity of the map, which means that, if $G = 1$, we must have $\sum_i S_i\,(t+1) = \sum_i S_i(t)$. This can be achieved in the following way: if a cell is near the boundary, so that according to the radius r, it lacks some neighbours, we assume that these neighbours exist and have the same intensity and capacity as the cell in question. The effect of this is equivalent to an increase in the coefficient λ in Equation 4 just for this particular cell. We prove in the Appendix that this construction effectively makes the total intensity constant in the absence of growth factors.

The map we have used contains a generous buffer around the study region and so the artificial treatment of the cells near the boundary has little influence inside the region.

2.2.6. Optimisation criteria

Since we only considered two possibilities for the kernel function f, the optimisation essentially concerns the other two parameters r and λ for each choice of f. Given that the conic-shaped function introduced above gave better results than the Gaussian kernel in the first experiment, we considered only the first choice. With f already fixed, two parameters remain, namely λ, which is within the interval $[0,1]$, and the positive radius r.

The calibration of the automaton must follow a criterion of discrepancy (or 'distance') between the predicted and the observed light intensities. We adopted the L^2-criterion (or least squares) applied to the last predicted year. If $S_i(r,\lambda)$ is the final predicted state for cell \$i\$ when using given values of (r,λ), and I_i is the real observed intensity of that cell, we can compute the loss function (eq. 5):

$$\text{Eq. 5} \qquad L(r,\lambda) = \sum_i (S_i(r,\lambda) - I_i)^2$$

Next, we want to find the specific values of (r,λ) that make L as small as possible.

The L^2-criterion is a loss function measuring the goodness of an approximation. It tends to penalise larger deviations more and to be more lenient with smaller ones. Another alternative sometimes used in statistics is the L^1-criterion, which gives a penalty proportional to the deviation, that is:

$$\sum_i |S_i(r,\lambda) - I_i|$$

The optimisation criterion is independent of all other modelling options and may be changed easily in any computational experiment.

The specific optimal value of $L(r,\lambda)$ has no natural interpretation in terms of the real data. It is just a measure of discrepancy or dissimilarity between two objects. The best way to visualise the goodness of the model obtained is to represent the distribution of the errors through all cells. We will show histograms of these distributions.

2.2.7. Optimisation algorithm

A first exploration of the value of the loss function L in the case of the studied NUTS-2 region showed that it is sufficient to search for values of (r,λ) inside the rectangle $[1,9] \times [0.5,1]$, since the loss function clearly gives larger values outside. It seems logical that the current light intensity of a cell influences its value the following year more than that of neighbouring cells because one year is too short a time in which to see large changes in the occupation and land use in the territory. Hence, it is enough to consider $\lambda \geq 0.5$. On the other hand, it seems that radii over 9 lead to larger values of the loss function unless λ is very close to 1, which means that the neighbourhood is not really playing any role in the prediction. A radius less than 1 means that the neighbourhood is practically non-existent.

The loss function depends in a very complicated way on the variables r and λ. To find its global minimum, we employed the Nelder-Mead algorithm in the version in the GNU Scientific Library, implemented in the C programming language. This algorithm does not need information about derivatives, which are not available in our case. Instead, it is fed with three non-aligned points in the plane, as a first guess of the region where we expect to find the minimiser (r,λ). Then this triangle of points evolves according to deterministic rules, moving, stretching and shrinking until its size is less than a given tolerance. The best point evaluated at that moment is outputted as the result of the algorithm (Nelder and Mead 1965).

The Nelder-Mead algorithm is a local search method. This means that there is no guarantee of finding the global optimum of a function in a given bounded domain unless the function behaves well. In general, the algorithm will get stuck at a local optimum, that is, a point with the minimum value in a circle (perhaps very

small) surrounding it. In fact, the algorithm can even stop at a point that is not near a local optimum depending on the tolerance set up as a stopping criterion.

Indeed, the preliminary exploration in our case study of Catalonia showed that even with a quite strict tolerance parameter, the algorithm stops at many different candidates for local minimum depending on the starting triangle. In view of this, we decided to start with a simple evaluation of the function on a grid covering the initial rectangle. The option to change the optimisation algorithm capable of performing a global search, e.g. Simulated Annealing, was deemed too costly in terms of computational time. Instead, the picture of the function highlights the promising regions where the global optimum could be located. We successively refined the evaluation grid and finally applied the Nelder-Mead algorithm again to restricted small regions.

2.2.8. Economic scenarios

Several studies have shown a strong relationship between NTL satellite data and socioeconomic parameters based on the assumption that there is light emission where there is population and economic activity (Doll 2008, Ghosh et al., 2010). In this study, we assumed that there is a linear relationship between the two variables 'light intensity' and 'Gross Domestic Product' (GDP) (Sutton et al. 2007, Marull et al 213). Therefore, we can predict the dynamics of space-time urban systems by taking into account different economic scenarios: i) business as usual (NTL trend continues), ii) economic expansion (NTL increase), or iii) economic contraction (NTL decrease).

Once we obtain the best possible values of r and λ, we can project ahead in time the evolution of the intensities using these best values. As has been mentioned above, the loss function has several local minima, some of which have values that are quite close to the global optimum. It is reasonable to expect that if two different pairs of values (r, λ) give a similar prediction error, then their projections will yield similar results. Nevertheless, this is a point that requires further computational checking.

We hypothesized three different scenarios for growth values. The first is the continuation of the tendency of the previous years, with the overall growth in the past 20 years being computed from the total intensities in 1992 and 2012:

$$G = \frac{\sum_i S_i(2012)}{\sum_i S_i(1992)}$$

To project 20 years ahead, steady annual growth is computed for every year so that the final overall growth coincides with G, which is simply $\sqrt[20]{G}$. The second scenario corresponds to an increase in the overall growth G by 5 percentual points (economic expansion), and the third to a decrease G by 5 percentual points (economic contraction).

3. Results and Discussion

3.1. Model calibration: European NUTS-2 Catalonia region

The raw data had certain problems and so we took the following actions: i) some cells had intensities in particular years that were greater than their theoretical capacity; in these cases, we augmented the capacity M_i to accommodate all recorded intensities; and ii) in general, in the evolution over time of a cell we observed great fluctuations in light intensity, many of which seemingly correspond to missing data that were filled in automatically; this results in a number of erratic ups and downs that do not appear to correspond to reality. We thus decided to smooth the data by interpolation when an increase or decrease in intensity in successive years is followed by a movement in the opposite direction (if the total fluctuation is greater than a fixed value). We established a fluctuation threshold of 15 intensity points; in all, there were 20,728 fluctuations, corresponding to 12,186 cells out of the total of 137,150.

The first experiments with the Nelder-Mead algorithm to find the optimal values of r and λ revealed the existence of many local minima in the loss function (eq. 5), approximately around a curve in the (r, λ)-plane. The optimisation process converges on any of these minima depending on the choice of the initial triangle of points (see Subsection 2.2.7). Since the optimisation is costly in terms of function evaluation (hence in terms too of the number of different CAs with different parameters that have to be run), it is better to invest computational resources in picturing directly the values of the function on a grid of a reasonable range of points as a first step. Six minutes in a dedicated processor Intel i7-8850U at 1.80Ghz and sufficient RAM memory was needed to compute the values of the loss function with radii varying from 1 to 9 with steps of 0.25, and λ from 0.55 to 0.975 with steps of 0.025.

We found that, in general, the bigger the radius, the bigger λ is required to achieve a low value for the loss

function. This has a natural interpretation: if we fix a large radius, thereby considering the influence of many distant cells, it is logical that the weight λ of the value of the cell itself will be greater to protect it against possibly irrelevant distant neighbours. Conversely, if we fix a small radius meaning that only proximate cells have an influence (given that this influence is possibly genuine), the weight of the central cell will be less. We should also bear in mind that the bigger the radius, the flatter the kernel function, which means that distant cells tend to contribute with a weight that is only slightly less than that of the closer ones.

In the extreme case when $\lambda = 1$, the CA does not play any role and the value of the loss function is, of course, independent of r, and yields $1{,}209.76$, rounded to two decimal places. Anything below this value, as we indeed obtained, means that the combination of the CA and the current value of the cell is a better predictor than the current value of the cell alone, thereby proving the usefulness of considering the spatial interaction.

A further finer grid was evaluated, with $r \in [2.0, 6.0]$, at steps of 0.1, and $\lambda \in [0.65, 0.95]$ at steps of 0.005, where the previous evaluation showed that loss function seemed to take lower values. It became clear that the loss function is very irregular and that it is not easy to locate the global minimum. There were 10 points with a value between $1{,}148$ and $1{,}149$ in this region, which correspond approximately to four disconnected regions in the (r, λ)-plane.

In view of the results of Table 1, we can affirm that there are different pairs of radii of influence and relative weights of the cell that yield similar results. As a general conclusion, it is clear that a radius of 2.5–4 km is a reasonable range for spatial influence, with a cell weight of 83–91%. The best pick is given by a radius of approximately 3.5 km and a 91% cell weight vs. a 9% cell weight influence of neighbouring cells.

A further zoom around the best point in each of the four disconnected regions gave a slightly better value $(1{,}146.41)$ for a radius of 3.18 km and cell weight of 91.13%. We take this point to be the absolute minimiser of the loss function. At the end of the time span of the prediction (year 2012), the discrepancy between the prediction and the real data for the optimal parameters is summarised in Fig. 3, with a description of the distribution of the errors. For instance, in $32{,}878$ of the 50,158 cells (65.55% of the cells), the prediction error in the light intensity lies between -3 and 3 intensity points, in 5360 cells the error is between 3 and 9 (overestimation), in 8276 between -9 and -3 (underestimation), and so on. Disregarding the central interval, a total of 6821 (13.60%) cells were overestimated, while $10{,}459$ (20.85%) were underestimated.

These results correspond to a prediction 20 years ahead in time since we used data from 1992, plus the growth in total illumination from one year to the next, to predict the illumination of each cell in 2012. Of course, better predictions will result if we reduce the time span. We repeated the above methodology to predict the values of 2012 starting from those of 1997 (15 years), 2002 (10 years) and 2007 (5 years). For the 15-year span, we obtained reasonably low values in the loss function for radii of 4.9– 5.7 km, with λ of 90– 92.5%. The best places form three disconnected (but close) spots; a further refinement and application of the Nelder-Mead algorithm gave the absolute best point with a radius of 4.99km and $\lambda = 90.30\%$, with a loss function value of 1052.50. For the 10-year span, reasonable values for the radius were 2.1–2.4km, and for λ 79– 81%, localised in two very nearby sites. Proceeding in the same way as before, we found the best values to be radius $= 2.35$km and $\lambda = 80.55\%$. Thus, in the 15-year prediction the radius decreases, with a corresponding decrease also in the importance of each cell with respect to the neighbourhood. The loss function becomes also more regular, with less local minima. When reducing the time span to just five years, we found only one spot of low loss values, very concentrated in radii around 1 or 1.1 km, but quite a wide spread in λ of 67.5– 73.5%. The best point found corresponds to radius $r = 1.00$km and $\lambda = 72.5\%$. Fig. 3 contains the error distributions for the 20-year span.

For the calculation of the scenarios in the NUTS-2 region of Catalonia, the overall growth factor in 1992–2012 was 1.118. The steady annual growth factor for obtaining this value in twenty years time (2032) is 1.005608. Under the contractive scenario (-5%) it is 1.003311, while for the expansive scenario ($+5\%$) it is 1.007809. In the case of the 15-year prediction (2027), the overall growth is 1.011, and the corresponding annual values are, respectively, 1.000709, 0.997330 and 1.003936; for the 10-year span (2022), the values are, respectively, overall 1.028, and annuals 1.002726, 0.997737 1.007501, while for the 5-year (2017), the values are, respectively, overall 0.954, and annuals 0.990699, 0.980093 and 1.000869.

3.2. Model application: European NUTS-3-based metropolitan regions

We applied the same methodology tested in the European NUTS-2 region of Catalonia to data from twelve European NUTS-3 metropolitan regions (Fig. 2) that, unlike the Catalan case, are small regions around big cities. The data lacks the lighting capacity of each cell and so we assumed for this study that all cells have a maximum capacity 63. We used a 20-year time span, with the following results:

i) *Amsterdam* (2032). The exploration of the best zones for the parameters r and λ gave a radius of 2.8–3.7 km and a λ of 63–73%. The discrepancy between the simulated and real data is similar in this range of values, with λ tending to increase as r increases, as in the case of Catalonia. Running the optimisation algorithm gave an optimal value at $r = 3.24$ km and $\lambda = 63.58\%$. ii) *Barcelona* (2032). The best values were 2–3.5km, with λ 30–75%. The absolute minimum is found at 2.38 km and $\lambda = 47.18\%$. Table 1 shows for this city all radii between 1 and 5 km and the best λ in a grid of resolution 0.05. iii) *Brussels* (2032). In this case, the optimal radius is much larger than in the previous two cases. Anything in the range 12–18 km was found to be a reasonable radius of influence, provided λ is kept consistently close to 54%. In this case, the rule that larger radii imply more cell weight does not seem to apply. The best point found was at $r = 16.97$ and $\lambda = 53.99$. iv) *Hamburg* (2032). As in the case of Brussels, the loss function continues to decrease as the radius increases. We reached our limit of 25km (the limit we imposed both for computational and modelling reasons) and the loss function still seems to give lower values beyond that limit. However, the decrease is very slow, and the parameter λ stabilises at around 90%. This means that better simulations are obtained with large radii with uniform neighbourhood influence with a weight of about 10% vs. the 90% of the cell itself. v) *London* (2032). Good results of similar quality are obtained for radii of 3–3.5 km, and λ of 50–56%. The best parameters were found at 3.11km and 54.69%. vi) *Lyon* (2032). As in the case of Brussels, the radii tend to be large but here λ also increases. Local optimisation around the 19-km mark gave the optimal pair $(r, \lambda) = (19.51, 0.9206)$. vii) *Madrid* (2032). As in the case of Hamburg, the loss function tends to prefer a very large radius of influence. Our limit of 25 km was reached, with an optimal λ of 72.99%. This means that about 37% of the prediction for the cell comes from a very large neighbourhood, with small and almost equal weights for all cells within a radius of 25 km. viii) *Milan* (2032). Similar to the cases of Hamburg and Madrid, we reached a radius $r =$ 25 km, with values of λ of 86–92% giving similar values. With a radius fixed at 25 km, the best λ found was 87.00%. ix) *Munich* (2032). Again the maximum radius of 25 km was optimal, with a $\lambda = 70.96\%$ similar to that of Madrid. x) *Rome* (2032). This city has the same pattern as Catalonia (increasing radius implies increasing λ). The range of good radii seems to be 1.75–3.00 km, with λ 30–70%. The loss function is very flat in all this rectangle. The absolute minimum is found at 2.18 km and $\lambda = 35.55\%$. This means that around 64% of the value of a cell 20 years later is explained by its surroundings at distances up to 2.18 km, and around 36% by the current value of the cell. xi) *Paris* (2032). The loss function decreases steadily as the radius grows. At $r =$

25 km, a wide range of λ values, 66–84%, give similarly low values. The absolute minimum found was at 76.58%, but the loss function was very flat for each fixed (large) radius. xii) *Vienna* (2032). Similar to Paris, here the optimal radius was large and the loss function keeps decreasing when it reaches 25 km. As in the other cases where this occurs, all surrounding cells in a wide neighbourhood tend to contribute similar weights. The coefficient λ tends to stabilise at around 82% for large radii. The absolute optimum for 25 km was found at $\lambda = 82.59\%$.

Fig. 4 depicts cartographically the results of applying the model to the twelve studied metropolitan regions. The continued trend scenario ('business as usual'), the expansive scenario (+5% NTL) and the regressive scenario (-5NTL) for each metropolitan region are shown. In general, an increase in *light intensity* and *illuminated surface* can be observed in the expansive scenario vs. the trend scenario, and a strong contraction of *light intensity* in the regressive scenario (Fig. 5). In the case of the *illuminated surface* variable (Fig. 5 shows DN>10), no major changes are visible (for example, in Brussels and Milan) because the studied metropolitan regions are already highly urbanized. Therefore, the model behaves as expected (Figs. 4 & 5), in the sense that it is sensitive to changes in any increase in NTL. As this parameter is related to an increase in GDP, we believe that the model allows us to calculate urban growth scenarios related to economic activity. Consequently, albeit with possible further improvements, the CA model developed from NTL satellite data would seem to be a good option for calculating metropolitan dynamics at regional level.

3.3. Model limitations and further improvements

One of the limitations of the model is related to the existence of a maximum illumination of the cells. Intuitively, we expect that the cells with more intensity 'contaminate' those with less intensity without losing intensity, hence to visualize the urban expansion as an expansion of the red zones in the maps of Fig. 4. But the conservation of total intensity (except for the growth factor) entails also a decrease in the intensity of the more illuminated cells. The growth factor is not enough to keep the intensity consistently at the maximum. This is of course more noticeable in the contraction scenarios. In any case, the cellular automaton has a diffusive effect, which is greater the radius of influence and lesser the coefficient λ. A value of λ close to 1 indicates that the cell resists the influence of the neighbourhood. In the NUTS-3 study, the diffusive effect can be noticed to a more or less extent. For instance, in the Catalan case, with λ=91%, the diffusion has a moderate effect.

A feature of the model is that very different values of the pair (r, λ) may give rise to similar low values of the loss function, when we are trying to find the optimal pair. This is somehow expected, because the radius of neighbourhood influence and the resilience to change of a cell are antagonist parameters. An increase in one of them can be compensated by an increase in the other. Of course, we took the best pair found in terms of the prediction obtained for the target year, and projected the scenarios using this optimal pair. Another simplification of the model is that the measure of the error (ordinary least squares) puts the same weight to all cells in its contribution to the total error. One could penalise more certain types of cells (those for which we want a better prediction), and obtain other optimal pairs (r, λ) that could project better the scenarios in those particular cells; or divide the region in classes of different typology (geographically or not) and obtain different (r, λ) for each class.

As mentioned above, one possible way of improving the CA model would be to localise the growth factor for regions smaller than the scope of this study, each with a different growth factor. For instance, in the case of Catalonia, although the study used $50{,}158$ cells, the growth factor is clearly not uniform throughout the whole territory. Instead of considering only the current state of the cell in its own contribution to the following year's value, we could also consider its evolution. The evolution of the each cell constitutes a time series from which a prediction can be extrapolated for the next year. For instance, we could consider the five previous years and use them to predict the value of the cell in the sixth year. This value can be used in our transition rule instead of the current value of the cell. Possibly, another parameter η could be introduced to allow some flexibility in the individual projection of each cell, thereby optimising jointly the three resulting parameters r, η and λ. Nevertheless, the time series is necessarily short and it is not clear what we would gain by introducing this new optimisation variable.

Despite the fact that our model considers separately the contribution of the cell itself and the contribution of the neighbourhood, this formalism can be focussed into a pure CA. With the extension proposed above, the model is no longer isomorphic to a CA. This would give a mixed model combining a time series evolution TS_i of the individual cell i – possibly depending on one or more parameters η – and a CA yielding a prediction CA_i, and depending on the radius parameter r by way of a convex combination parameter λ. The new state of the cell i, given the whole map at time t, would be:

$$S_i(t+1) = \lambda TS_i(t+1) + (1-\lambda)CA_i(t+1)$$

If the predictions TS_i and CA_i are constructed to respect the bounds 0 and M_i of the cell intensity, the convex combination will, of course, respect these limits. There is no guarantee, however, that the total intensity will be preserved (in the absence of a growth factor) unless a compensation mechanism is put into place. Only if such a mechanism is designed and well justified from a modelling point of view will it be worth trying this extension.

4. Conclusion

The goal of this paper was to use NTL satellite imagery from twelve NUTS-3 European metropolitan regions (*Amsterdam*, *Barcelona*, *Brussels*, *Hamburg*, *London*, *Lyon*, *Madrid*, *Milan*, *Munich*, *Paris*, *Rome* and *Vienna*) and historical data to develop a method for calibrating a mathematical CA model and predict urban scenarios. The resulting transition rules were not stochastic or distance-decay-dependent, as expected in urban systems (White and Engelen 2000), but were dependent on the previous states of a cell's neighbours. In order to calibrate and validate the model with real data (Engelen and White 2008), we used NTL data for the years 1992–2012 from the NUTS-2 region of Catalonia. The *lighted surface* scenario (as a proxy of urban expansion) was given by variations in *light intensity* (as a proxy of economic activity) imposed exogenously (Ghosh et al., 2010). The CA model behaved as expected and was sensitive to changes in the increase in NTL. As this parameter is related to the increase in GDP (Sutton et al. 2007), we believe that the model allows us to calculate urban growth scenarios based on economic activity. Consequently, with possible further improvements, the CA model developed from NTL satellite data would seem to be a good option for calculating metropolitan dynamics at regional level.

Since NTL is available for the whole planet, this CA model could be used to study urbanisation dynamics in many regions including, in particular, those for which socio-economic data are not available (Zhang and Seto 2011) and emerging metropolis and megaregion global economic units (Marull et al. 2013). We used an inverse and heuristic approach based on data analysis to develop a new urban CA-based model with coarse cell size (Rabino and Laghi 2002) defined by NTL satellite data. In a previous work (Chowdhury and Maithani, 2014) using another type of data, we considered a CA-based model related to NTL but with a simple on-off viewpoint. Our model gives us three kinds of useful approximate information related to urban surface areas: the main one is a NTL urban surface baseline, which in turn was used in the calibration and validation processes; the second

one is a regression line for the NTL intensity and GDP, which arguably could be improved with further research; finally, we found a good coarse approximation to urban shape in urban progress scenarios.

Future usage of these outputs relies on the fact that NTL occurs over the entire planet. Therefore, it is to be expected that our CA model and any further improvements will be useful for studying urbanisation dynamics in other metropolitan regions, above all in those for which socio-economic data are not available, and for assessing the sustainable progress of urban networks (Marull et al. 2019). Our model could be improved using an integrated approach that includes GIS and Dynamical System components if required data exists.

References

Allen PM. 1997. Cities and Regions as Self-Organizing Systems: Models of Complexity. Taylor and Francis, London.

Al-shalabi M, Billa L, Pradham B, et al. 2013. Modelling urban growth evolution and land-use changes using GIS based cellular automata and SLEUTH models: the case of Sana'a metropolitan city, Yemen. Environmental Earth Science 70, 425-437. https://doi.org/10.1007/s12665-012-2137-6.

Arcaute E, Hatna E, Ferguson P, et al. 2015. Constructing cities, deconstructing scaling laws. Journal of the Royal Society Interface 12, 20140745. https://doi.org/10.1098/rsif.2014.0745.

Barreira-González P, Aguilera-Benavente F, Gómez-Delgado M. 2015. Partial validation of cellular automata based model simulations of urban growth: An approach to assessing factor influence using spatial methods. Environmental Modelling and Software 69, 77-89. https://doi.org/10.1016/j.envsoft.2015.03.008.

Batty M. 2005. Cities and Complexity: Understanding Cities with Cellular Automata, Agent-Based Models, and Fractals. Cambridge, MA: MIT Press.

Batty M. 2011. Commentary: When all the world's a city. Environment and Planning A 43, 765-772. https://doi.org/10.1068/a43403.

Batty M. 2015. Models again: their role in planning and prediction. Environment and Planning B 42, 191-194. https://doi.org/10.1068/b4202ed.

Benenson I. 1999. Modeling population dynamics in the city: from a regional to a multi-agent approach. Discrete Dynamics in Nature and Society 3, 149-170. http://dx.doi.org/10.1155/S1026022699000187.

Benenson I, Torrens PM. 2004. Geosimulation: Automata-Based Modeling of Urban Phenomena. John Wiley & Sons Ltd.

Chowdhury P, Maithani S. 2014. Modelling urban growth in the indo-gangetic plain using nighttime ols data and cellular automata. International Journal of Applied Earth Observation and Geoinformation 33, 155-165. http://dx.doi.org/10.1016/j.jag.2014.04.009.

Clarke K, Hoppen S, Gaydos L. 1997. A self-modifying cellular automaton model of historical urbanization in the San Francisco bay area. Environment and Planning B 24, 247-261. https://doi.org/10.1068/b240247.

Couclelis H. 1985. Cellular worlds: a framework for modeling micro-macro dynamics. Environment and Planing A 17, 585-596. https://doi.org/10.1068/a170585.

Doll C. 2008. Thematic Guide to Night-time Light Remote Sensing and its Applications. Centre for International Earth Science Information Network (CIESIN), Columbia University, New York.

Engelen G, White R. 2008. Validating and Calibrating Integrated Cellular Automata Based Models of Land Use Change. In Albeverio S, Andrey D, Giordano P, Vancheri P (eds.). The Dynamics of Complex Urban Systems. Physica-Verlag, Heidelberg.

Gardner, M. 1970. Mathematical Games – The fantastic combinations of John Conway's new solitaire game "life". Scientific American 223 (4), 120-123. https://web.stanford.edu/class/sts145/Library/life.pdf.

Ghosh T, Powell R.L, Elvidge CD, et al. 2010. Shedding light on the global distribution of economic activity. The Open Geography Journal 3, 148–161. https://doi.org/10.2174/1874923201003010147.

Guan D, Li H, Inohae T, et al. 2011. Modeling urban land use change by the integration of cellular automaton and Markov model. Ecological Modelling 222, 3761-3772. https://doi.org/10.1016/j.ecolmodel.2011.09.009.

Liu Y. 2009. Modelling Urban Development with Geographical Information Systems and Cellular Automata. CRC Press.

Ioannides YM. 2012. From Neighborhoods to Nations: The Economics of Social Interactions. Princeton University Press.

Marull J, Galletto V, Domene E, et al. 2013. Emerging megaregions: a new spatial scale to explore urban sustainability. Land Use Policy 34, 353-366. https://doi.org/10.1016/j.landusepol.2013.04.008.

Marull J, Font C, Boix R. 2015. Modelling urban networks at mega-regional scale: are increasingly complex urban systems sustainable? Land Use Policy 43, 15–27. https://doi.org/10.1016/j.landusepol.2014.10.014.

Marull J, Farré M, Boix R, et al. 2019. Modelling urban networks sustainable progress. Land Use Policy 85, 73-91. https://doi.org/10.1016/j.landusepol.2019.03.038.

Nelder JA, Mead R. 1965. A Simplex Method for Function Minimization. The Computer Journal 7 (4), 308-313. https://doi.org/10.1093/comjnl/7.4.308.

Nel·lo O, López J, Martín J, et al. 2017. Energy and urban form. The growth of European cities on the basis of night-time brightness. Land Use Policy 61, 103-112. https://doi.org/10.1016/j.landusepol.2016.11.007.

Portugali J. 2000. Self-Organization and the City. Springer.

Portugali J. 2011. Complexity, Cognition and the City. Physica-Verlag, Heidelberg.

Rabino GA, Laghi A. 2002. Urban Cellular Automata: The Inverse Problem. In Bandini S, Chopard B and Tomassini M (eds.). Cellular Automata, ACRI 2002. Springer-Verlag, 349-356. https://doi.org/10.1007/3-540-45830-1_33.

Rai V, Robinson SA. 2015. Agent-based modeling of energy technology adoption: Empirical integration of social, behavioral, economic, and environmental factors. Environmental Modelling and Software 70, 163-177. https://doi.org/10.1016/j.envsoft.2015.04.014.

Santé I, Garca AM, Miranda D, Crecente R. 2010. Cellular automata models for the simulation of real-world urban processes: A review and analysis. Landscape and Urban Planning 96, 108-122. https://doi.org/10.1016/j.landurbplan.2010.03.001.

Sutton P, Elvidge C, Ghosh T, 2007. Estimation of gross domestic product at subnational scales using nighttime satellite imaginary. International Journal of Ecological Economics and Statistics 8, 5-1.

Van der Leeuw S.E. 2004. Why model? Cybernetics and Systems: An International Journal 35, 117-128. https://doi.org/10.1080/01969720490426803.

Van Vliet J, Hunkens J, White R, Van Delden H. 2012. An activity-based cellular automaton model to simulate land-use dynamics. Environment and Planning B 39, 198-212. https://doi.org/10.1068/b36015.

White R. 2006. Modeling Multi-scale Processes in a Cellular Automata Framework. In Portugali J (ed.).

Complex Artificial Environments. Springer-Verlag, 165-177. https://doi.org/10.1007/3-540-29710-3_11.

White R, Engelen G. 1997. Cellular automata as the basis of integrated dynamic regional modelling. Environment and Planning B 24, 235-246. https://doi.org/10.1068/b240235.

White R, Engelen G. 2000. High-resolution integrated modelling of the spatial dynamics of urban and regional systems. Computers, Environment and Urban Systems 24, 383-400. https://doi.org/10.1016/S0198-9715(00)00012-0.

Zhang Q, Seto K. 2011. Mapping urbanization dynamics at regional and global scales using multi-temporal dmsp/ols nighttime light data. Remote Sensing of Environment 115, 2320-2329. https://doi.org/10.1016/j.rse.2011.04.032.

Figures

Fig. 1 European NUTS-2 region of Catalonia used for model calibration. Night-Time Light (NTL) real evolution over space and time (1992, 1998, 2005 and 2012).

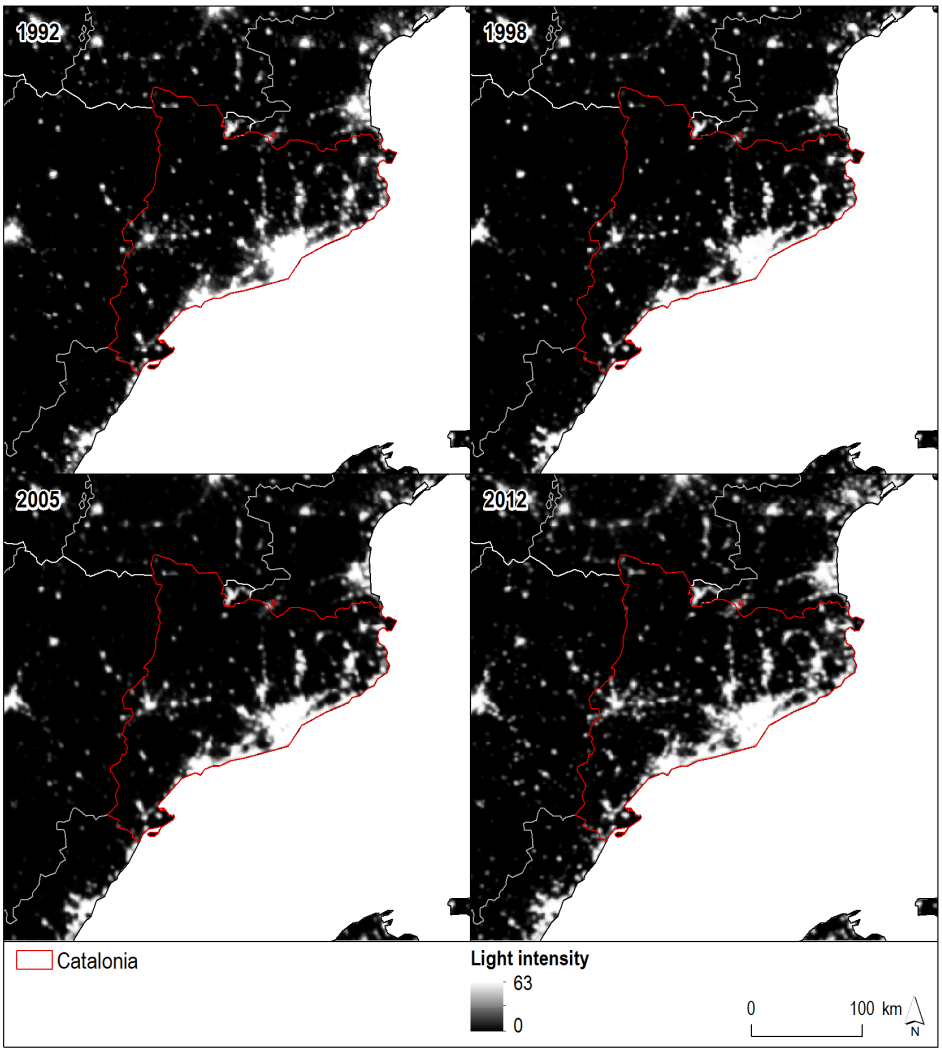

Fig. 2 The twelve European NUTS-3 metropolitan regions (*Amsterdam*, *Barcelona*, *Brussels*, *Hamburg*, *London*, *Lyon*, *Madrid*, *Milan*, *Munich*, *Paris*, *Rome* and *Vienna*) used for modelling the application. Night-Time Light (NTL) real evolution over space and time (1992, 1998, 2005 and 2012).

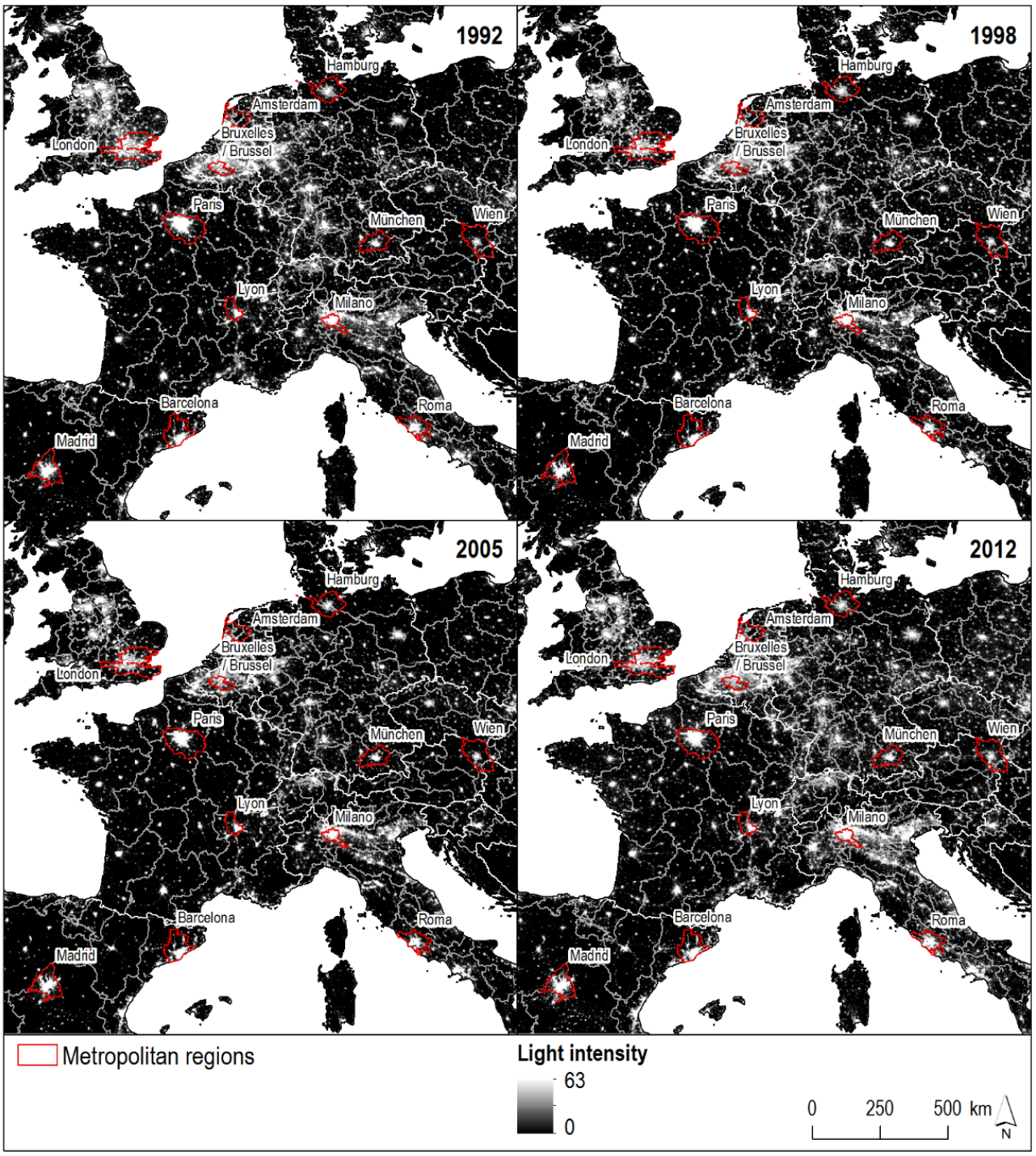

Fig. 3 Discrepancy between the prediction and the real data in the optimal parameters found in the case study of the European NUTS-2 region of Catalonia (20-year prediction: 1993–2012).

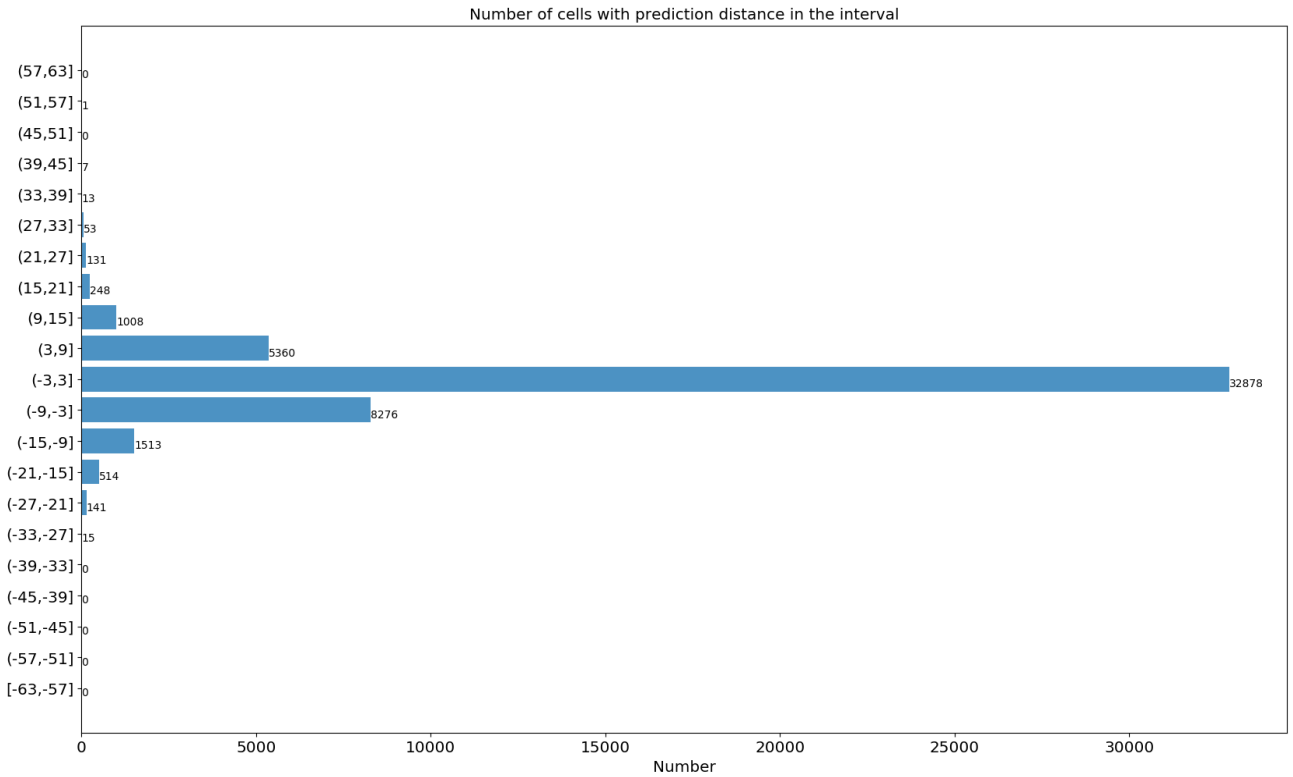

Fig. 4 Modelling results for the twelve European NUTS-3 metropolitan regions (*Amsterdam*, *Barcelona*, *Brussels*, *Hamburg*, *London*, *Lyon*, *Madrid*, *Milan*, *Munich*, *Paris*, *Rome*, and *Vienna*). Night-Time Light (NTL) economic scenarios (2032): continued trend scenario (business as usual), expansion scenario (+5% NTL) and contraction scenario (−5% NTL).

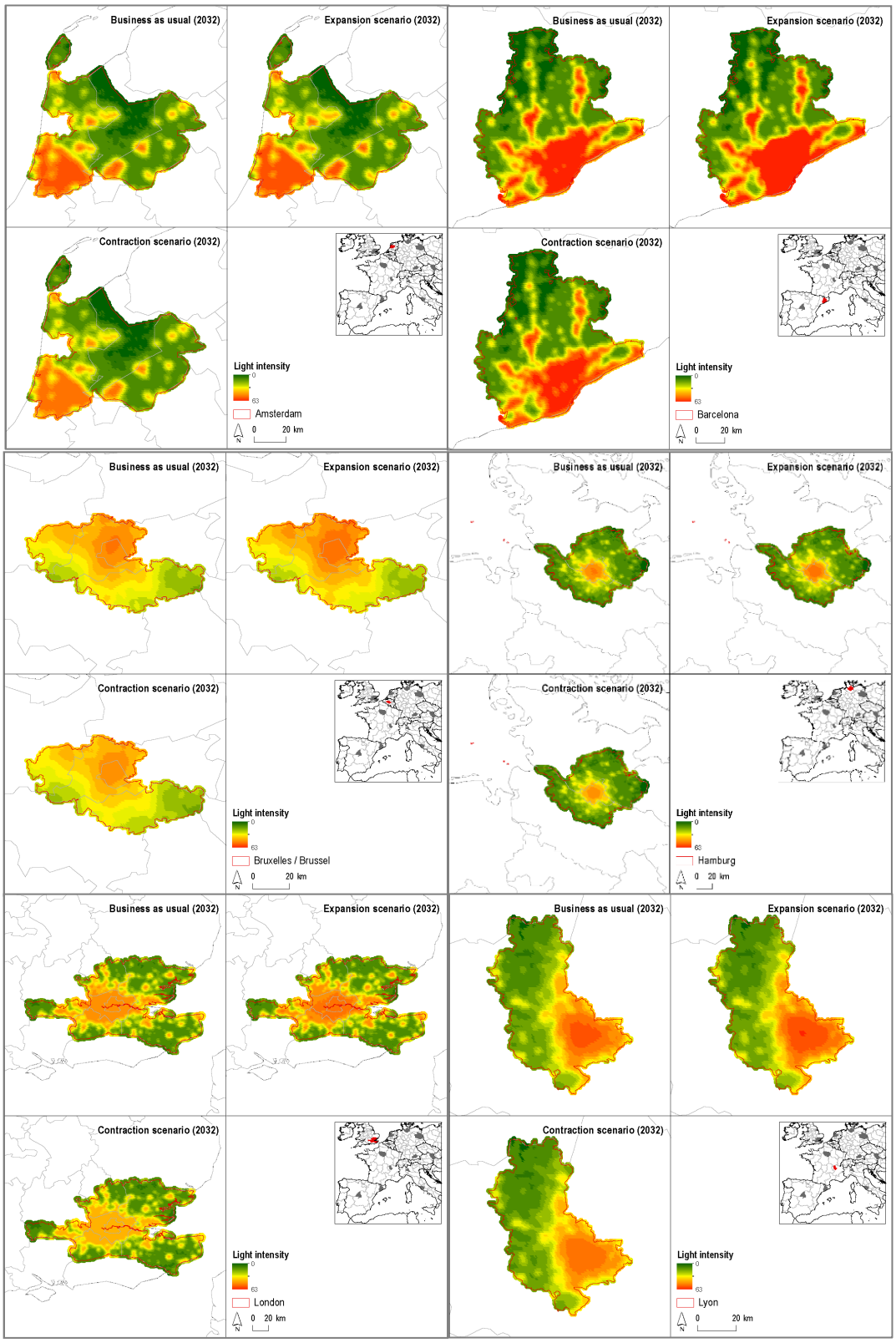

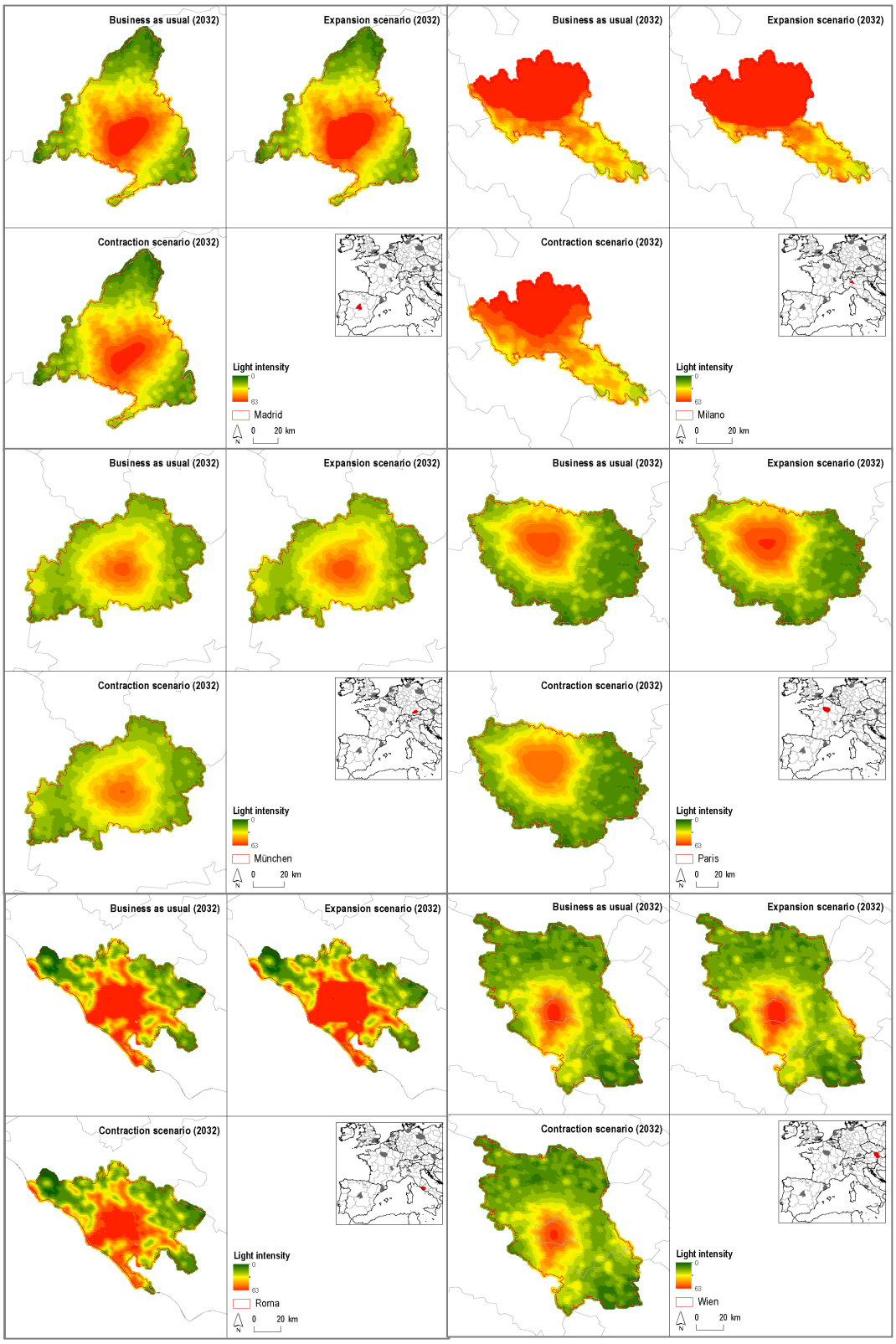
Business as usual (2032)
Expansion scenario (2032)
Business as usual (2032)
Expansion scenario (2032)
Contraction scenario (2032)
Contraction scenario (2032)
Light intensity
0
63
Madrid
0 20 km
Light intensity
0
63
Milano
0 20 km
Business as usual (2032)
Expansion scenario (2032)
Business as usual (2032)
Expansion scenario (2032)
Contraction scenario (2032)
Contraction scenario (2032)
Light intensity
0
63
München
0 20 km
Light intensity
0
63
Paris
0 20 km
Business as usual (2032)
Expansion scenario (2032)
Business as usual (2032)
Expansion scenario (2032)
Contraction scenario (2032)
Contraction scenario (2032)
Light intensity
0
63
Roma
0 20 km
Light intensity
0
63
Wien
0 20 km

Fig. 5 Application of the Cellular Automata (CA) model to twelve European NUTS-3 metropolitan regions. Night-Time Light (NTL) variables: *lighted surface* (km^2 as a proxy of urban expansion) and *light intensity* (sum of DN as a proxy of economic activity). Predicted economic scenarios (2032): continued trend scenario (business as usual), expansive scenario (+ 5% NTL) and regressive scenario (-5% NTL).

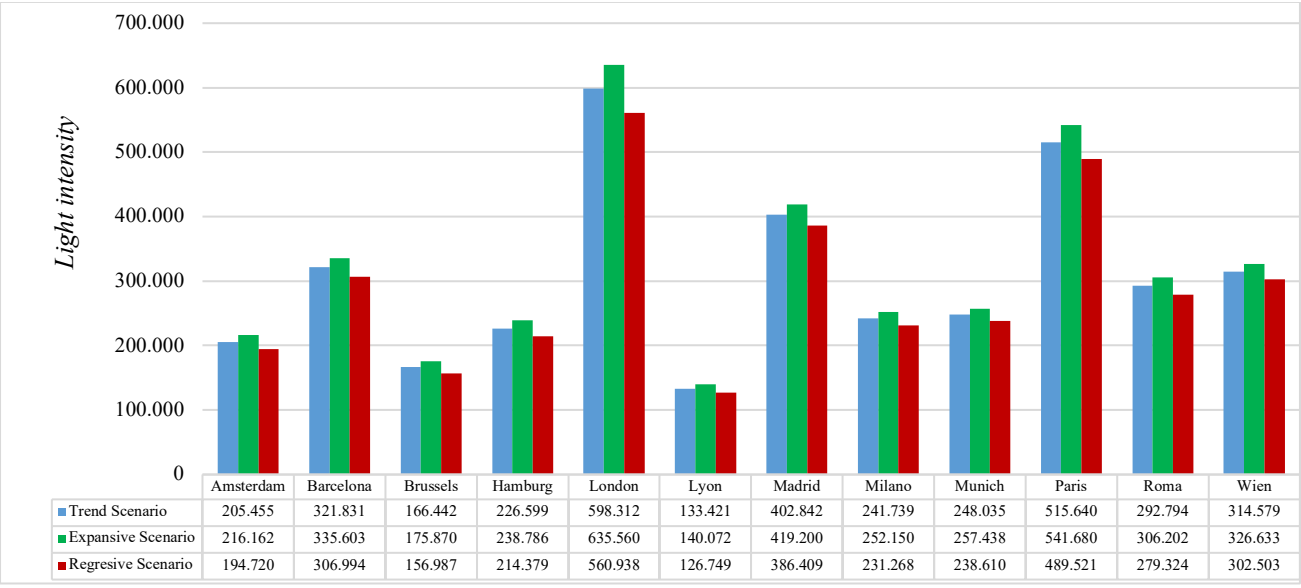

	Amsterdam	Barcelona	Brussels	Hamburg	London	Lyon	Madrid	Milano	Munich	Paris	Roma	Wien
Trend Scenario	205.455	321.831	166.442	226.599	598.312	133.421	402.842	241.739	248.035	515.640	292.794	314.579
Expansive Scenario	216.162	335.603	175.870	238.786	635.560	140.072	419.200	252.150	257.438	541.680	306.202	326.633
Regresive Scenario	194.720	306.994	156.987	214.379	560.938	126.749	386.409	231.268	238.610	489.521	279.324	302.503

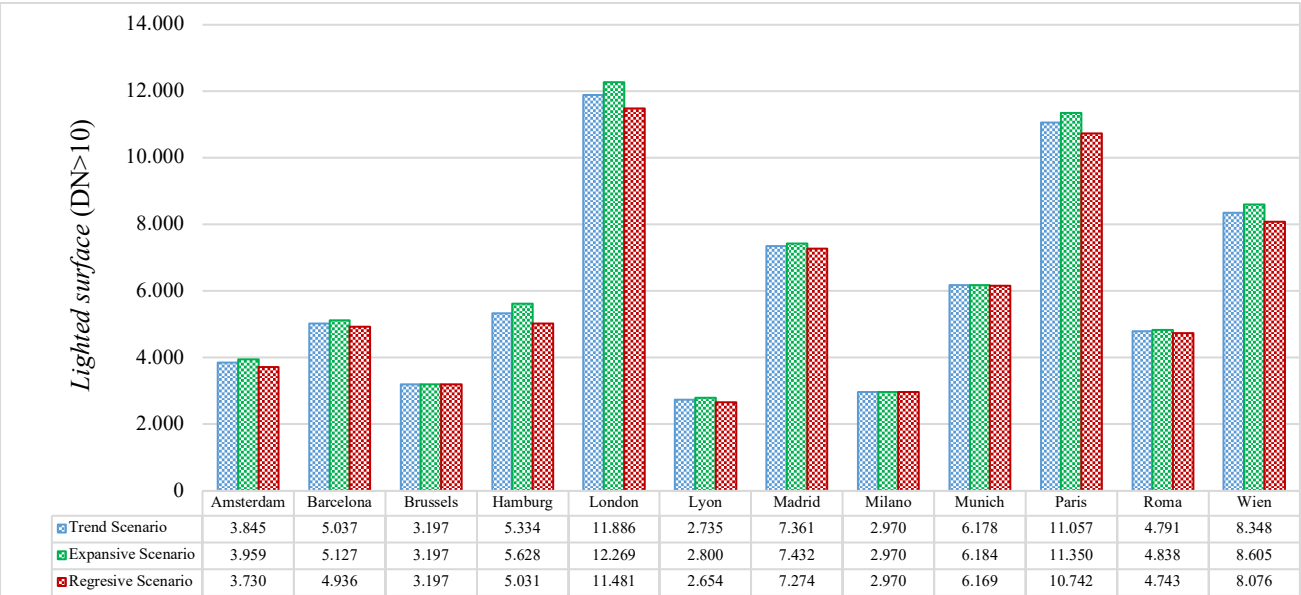

	Amsterdam	Barcelona	Brussels	Hamburg	London	Lyon	Madrid	Milano	Munich	Paris	Roma	Wien
Trend Scenario	3.845	5.037	3.197	5.334	11.886	2.735	7.361	2.970	6.178	11.057	4.791	8.348
Expansive Scenario	3.959	5.127	3.197	5.628	12.269	2.800	7.432	2.970	6.184	11.350	4.838	8.605
Regresive Scenario	3.730	4.936	3.197	5.031	11.481	2.654	7.274	2.970	6.169	10.742	4.743	8.076

Tables

Table 1 Model calibration in the NUTS-2 region of Catalonia and the Barcelona NUTS-3 metropolitan region. For each radius (km), the best λ in a 0.05-resolution grid is given.

Catalonia NUTS-2 region		
Radius (km)	Best **λ**	Loss function
2.50	0.835	1,148.69
2.50	0.840	1,148.95
2.60	0.835	1,148.74
2.70	0.830	1,148.62
2.70	0.835	1,148.53
3.10	0.870	1,148.53
3.20	0.875	1,148.91
3.50	0.910	1,148.96
3.50	0.915	1,148.97
3.90	0.875	1,148.99
Barcelona NUTS-3 region		
Radius (km)	Best **λ**	Loss function
1.00	0.30	1,311.47
1.25	0.30	1,310.90
1.50	0.30	1,310.28
1.75	0.30	1,309.42
2.00	0.30	1,308.08
2.25	0.40	1,308.08
2.50	0.50	1,307.97
2.75	0.60	1,308.28
3.00	0.65	1,308.31
3.25	0.70	1,308.53
3.50	0.75	1,308.93
3.75	0.80	1,309.27
4.00	0.80	1,309.72
4.25	0.80	1,310.37
4.50	0.85	1,310.88
4.75	0.85	1,311.14
5.00	0.85	1,311.77

Appendix

In this appendix, we provide a proof that the evolution of light intensities according to Eq. 3 preserves the total intensity of the map. Precisely, if $S_i(t)$ is the state (light intensity) of cell i at time t, then $\sum_i S_i(t+1) = \sum_i S_i(t)$, where the sum extends over all cells on the map. First, we can reduce the problem to ensure that the CA contribution C_i satisfies $\sum C_i(t) = \sum S_i(t)$. Assuming this is true, then $\sum_i S_i(t+1) = \lambda \sum_i S_i(t) + (1-\lambda)\sum_i S_i(t) = \sum_i S_i(t)$. According to Eq. 2 we need to show that

$$\sum_i \sum_{j \in N_i} w_j(i)\left(p_j(t) - p_i(t)\right)\left|S_j(t) - S_i(t)\right|$$

$$\wedge \left(M_i - S_i(t)\right) \wedge S_j(t) \vee -\left(M_j - S_j(t)\right) \vee -S_i(t) = 0$$

Let's disregard for a moment the existence of a boundary. Note that by interchanging the role of i and j in the summands, we obtain the same quantity with the sign reversed, one multiplied by $w_j(i)$ and the other by $w_i(j)$. However, these two values are the same: recall that the kernel function f has rotational symmetry. If we now call $(0,0)$ the central cell and (a,b) the cell located a places to the right and b places above the central cell, and we write $w(a,b)$ as its assigned weight, the symmetry implies in particular that $w(a,b) = w(-a,-b)$. And it is clear that if the relative position of cell i with respect to j is (a,b), then the relative position of j with respect to i is $(-a,-b)$. In conclusion, $w_i(j) = w_j(i)$.

Now, still disregarding the existence of a boundary, if i belongs to the neighbourhood of j, then j belongs to the neighbourhood of i, because the function f is the same throughout the map. This means that, in the double sum above, for every occurrence of a term starting with $w_j(i)$, there is another term starting with $w_i(j)$, which contributes the same quantity but with the sign reversed. The overall summation must therefore be equal to zero.

We still need to deal with the boundaries. The key points in the argument of the previous two paragraphs are that the relative positions of every pair of cells i and j can be considered to be the same and that both should appear on the map. When we take a cell near the boundary, we pad out the map with the missing cells to complete its neighbourhood and we give these artificial cells the same value as the original cell. The contribution $w_j(i)$ of the artificial cell j, that does not have a corresponding term $w_i(j)$, is therefore 0. This completes the proof.